Authors' last version, published in Chemical Engineering Science 137 (2015) 572-582

An Extended Corresponding States Equation of State (EoS) for CCS Industry

Mohamed Ibrahim[a,*], Geir Skaugen[b], Ivar S. Ertesvåg[a]

[a] *Department of Energy and Process Engineering, Norwegian University of Science and Technology, Kolbjørn Hejes veg 1B, NO-7491 Trondheim, Norway.*
[b] *SINTEF Energy Research, Trondheim, Norway*

Abstract

For a good design of all the processes in Carbon Capture and Storage, the thermodynamics of the CO_2 and CO_2 mixtures should be accurately predicted. Among these mixtures are CO_2-water systems that are very difficult to deal with due to the polar nature. In this work we suggest a new extended corresponding states equation of state (EoS) that can handle polar mixtures. The new EoS uses the Bender Modified Benedict-Webb-Rubin EoS as a reference equation. NH_3, R23 and R503 are used as reference fluids with parameters from Polt. The EoS presented uses the Soave-Redlich-Kwong EoS with Huron Vidal mixing rules based approach to compute the scale factors. The evaluation of the new EoS is done over a large set of experimental data. The results show very high accuracy in predicting both phase equilibrium and densities.

Keywords: Cubic EoS, Extended Corresponding States, MBWR EoS, CCS, Reference fluid, VLE.

*Corresponding author. Phone: +47 735 93841
Email addresses: mohamed.ibrahim@ntnu.no (Mohamed Ibrahim), Geir.Skaugen@sintef.no (Geir Skaugen), ivar.s.ertesvag@ntnu.no (Ivar S. Ertesvåg)

1. Introduction

There are a number of impurities in mixture with CO_2 that are relevant for the Carbon Capture and Storage (CCS) industry. Among these are H_2O, H_2S, CH_4, CO, O_2, NO_2 and N_2. The availability of the thermodynamic and transport properties of these mixtures is then vital for the design of various CCS processes. The experimental data are highly important. However, they are discrete in nature and local. Therefore, a generic and continuous solution is essential. Hence, modeling transport and thermodynamic properties of CO_2 with impurities is crucial for design, safety, efficiency and economy of the process.

It is possible to use empirically fitted models, but these models always have poor extendability and generality outside the fitted range. Moreover, they are not thermodynamically consistent over phases. A more appropriate and physically grounded approach is to use equations of state (EoSs). There are various categories of EoSs. Cubic EoSs like Soave-Redlich-Kwong (SRK) (Soave, 1972), SRK with Huron Vidal mixing rules (SRK-HV) (Huron and Vidal, 1979) and Peng–Robinson (PR) (Peng and Robinson, 1976) are amongst the lightest in computations. Consequently, they are the most widely used in industry. Among the heaviest in computation time are the full extended corresponding states (ECS) equations. A modern approach that is less computationally expensive than ECS, and offers generally good accuracy, is the multi parameters approach. Nevertheless, it is at least one order of magnitude higher than Cubic EoS in computation time (Wilhelmsen et al., 2012). Span–Wagner (Span and Wagner, 1996) for pure CO_2 and GERG (Groupe Européen de Recherches Gaziéres) (Kunz et al., 2007) for mixtures belong to this category. The Cubic-Plus-Association

(CPA) (Kontogeorgis et al., 1996) and the Statistical Associating Fluid Theory (SAFT) (Chapman et al., 1990) EoSs are state-of-the-art approaches. The results of the CPA and Perturbed Chain SAFT (PC-SAFT) for modeling CO_2-water systems were presented by Tsivintzelis et al. (2011) and Diamantonis and Economou (2012), respectively. The two articles also included a literature survey on CPA and SAFT type developments and recent achievements.

SPUNG EoS (Jørstad, 1993) is not a well known ECS equation although it handles the trade-off between accuracy and complexity well. The SPUNG EoS was first introduced for hydrocarbons. Recently Wilhelmsen et al. (2012) showed that SPUNG is a promising EoS for modeling CO_2 non-polar mixtures. However, we showed (Ibrahim et al., 2012, 2014b) that the SPUNG EoS qualities did not fully hold for modeling CO_2-water densities and phase equilibrium over large range of conditions. This is mainly for water-rich phase density predictions and CO_2 solubilities at all tested pressures. We also investigated the effect of reference fluid on the density predictions, and found that for the set of tested hydrocarbons as reference fluids, the heavier the hydrocarbon the better it predicted the water-rich phase density. Moreover, the study recommended development of asymmetric or non-quadratic mixing rules for better modeling of phase equilibrium (Ibrahim et al., 2014a,b). Mollerup (1998) earlier discussed generally the possibility of introducing non-quadratic mixing rules. However, he did not provide detailed derivations of specific mixing rule derivatives, or introduce a concrete model results. Furthermore, his general suggestions were incompatible with the implementation using van der Waals quadratic mixing rule. Therefore, they were not followed here. A similar discussion is made by Michelsen and Mollerup (2007).

Here, we introduce a new original ECS EoS that uses SRK EoS and HV mixing rules for the computation of the scale factors. The new equation uses the Bender Modified Benedict-Webb-Rubin (MBWR) EoS parameters by Polt (1987) as the reference equation. The results using three alternative reference fluids that exhibited the best compromise for phase equilibrium and density predictions are demonstrated.

2. Theory

2.1. Equations of state

An EoS is a model that calculates for both the liquid and gas phase using the same expression. This enhances the continuity near the critical point. An EoS for an N_c component mixture can be regarded as an expression for pressure P as a function of the mole fractions x_i, the temperature T and the volume V. Given this expression, the Helmholtz residual function ${A_\mathrm{m}}^\mathrm{res}[V,T,x]$, or the departure function $F = {A_\mathrm{m}}^\mathrm{res}[V,T,n]/(n_i RT)$, can be computed. Here, n is the amount of substance, R is the gas constant and subscript m stands for mixture. The thermodynamic properties can then be computed from the derivatives of the departure function as explained by Jørstad (1993) or most thermodynamics textbooks concerned with EoSs.

2.2. The corresponding states principle

The principle of corresponding states assumes that all substances exhibit the same behavior at a reduced state. Consequently, the departure function can be written for a pure component as

$$\frac{{A_i}^\mathrm{res}[V,T]}{n \cdot R \cdot T} = \frac{{A_\mathrm{Ref}}^\mathrm{res}[V_\mathrm{Ref}, T_\mathrm{Ref}]}{n \cdot R \cdot T_\mathrm{Ref}}, \tag{1}$$

or for a mixture as

$$\frac{{A_{\mathrm{m}}}^{\mathrm{res}}[V,T,x]}{n\cdot R\cdot T}=\frac{{A_{\mathrm{Ref}}}^{\mathrm{res}}[V_{\mathrm{Ref}},T_{\mathrm{Ref}}]}{n\cdot R\cdot T_{\mathrm{Ref}}}, \tag{2}$$

where index i denotes component, and subscript m stands for mixture.

A corresponding state EoS typically has one or more reference components described very accurately by a reference EoS. In the corresponding states approach, the reference fluid volume V_{Ref} and temperature T_{Ref} are the reduced volume and temperature, V_{R} and T_{R}, of the fluid or the mixture investigated. Here, subscript R and Ref stand for reduced and reference, respectively.

2.3. The extended corresponding states principle

2.3.1. Basic concept

In the extended corresponding states principle, the same principle is assumed. However, the mapping between the investigated fluid or mixture T and V and the reference fluid V_{Ref} and T_{Ref} is done via the scale factors f_{n} and h_{n} as

$$T_{\mathrm{Ref}}=\frac{n\cdot T}{f_{\mathrm{n}}}, \tag{3}$$

$$V_{\mathrm{Ref}}=\frac{V}{h_{\mathrm{n}}}. \tag{4}$$

These scale factors take into account how the fluids or the mixture in consideration differ from the reference fluid. As explained in Sect. 2.1, the thermodynamic properties are computed from the derivatives of the F function. Therefore, from the definition of F, formulations for f_{n} and h_{n} and their derivatives are needed. The scale factors, f_{n} and h_{n}, can be computed via

scale factor functions, using semi-empirical functions, an accurate reference equation for each component, or using a simpler EoS. The work on shape factor functions started by Leach et al. (1968). Subsequently, many contributions were made. Examples are the work by Fisher and Leland (1970) and of Ely (1990), who has introduced the first exact shape factor concept. In addition, a substantial work on shape factor functions was conducted by Estela-Uribe and Trusler (1998). The computation of exact shape functions is computationally very expensive because they are implicit functions of the reference fluid V_{Ref} and T_{Ref}. This is why the concept was left behind and thought to be impractical for use with numerical simulations. However, several implementations of the concept of extended corresponding states use simpler equations of state to compute shape factors and formulation that is independent of V_{Ref} and T_{Ref}, which showed a good compromise between accuracy and computation time. Among these are the SPUNG EoS that uses SRK EoS for the computation of the shape factors. The SRK EoS used in SPUNG EoS uses Soave's formulation for the computation of $\alpha(T)$ that appears in the equation of computing the a_i parameter of pure components,

$$a_i = a_i^{\mathrm{C}} \cdot \alpha(T). \tag{5}$$

Here, a_i^{C} is the parameter a for the pure component i at critical conditions.

Using SRK EoS with Soave's formulation for $\alpha(T)$, Jørstad (1993) showed that f_{n} and h_{n} can be defined, respectively, as

$$f_{\mathrm{n}} = \left(\frac{\sqrt{\frac{a_{\mathrm{n}}}{a_{\mathrm{Ref}}^{\mathrm{C}} \cdot h_{\mathrm{n}}}} + m_{\mathrm{Ref}} \cdot \sqrt{\frac{n \cdot T}{T_{\mathrm{Ref}}^{\mathrm{C}}}}}{1 + m_{\mathrm{Ref}}} \right)^2 \tag{6}$$

and

$$h_{\mathrm{n}} = \frac{b_{\mathrm{n}}}{b_{\mathrm{Ref}}}, \tag{7}$$

where

$$m_{\mathrm{Ref}} = \lambda + \beta \ \cdot \ \omega_{\mathrm{Ref}} - \gamma \ \cdot \ \omega_{\mathrm{Ref}}^2 \tag{8}$$

and λ, β and γ are constants that vary with the type of cubic EoS (e.g. 0.480, 1.574, and 0.176, respectively, for SRK). ω_{Ref} is the acentric factor of the reference component. The superscript C means at critical conditions, and the subscript n means molar based. A similar discussion is made by Mollerup (1998) and Michelsen and Mollerup (2007).

From Eqs. 6 and 7 it is clear that to compute the derivatives of f_{n} and h_{n}, a closure mixing rule formulation for the parameter a_{n} and its derivatives are needed. The mixing rule to be selected or developed must be thermodynamically consistent.

2.3.2. The new EoS

In the new EoS we first introduce here, the Bender-MBWR EoS with 20 parameters of Polt (1987) was used for the reference fluid. The reference fluids recommended here are R23, R503 and NH_3. The R23 is CHF_3, and R503 is a mixture of R23 and R13 ($CClF_3$). The reference fluids are recommended after investigating several reference fluids including O_2, N_2, water, CO_2, C1 to C9, and a set of refrigerants. Moreover, the cubic SRK-HV EoS was used to calculate the a parameter in the scale factors. The parameter a using Huron-Vidal mixing rules (Huron and Vidal, 1979) is defined as

$$a = b \left(\sum_{i=1}^{N_c} \left(x_i \frac{a_i}{b_i} \right) - \frac{G_{\infty}^{\mathrm{E}}}{\ln(2)} \right), \tag{9}$$

where b is the co-volume parameter defined as

$$b = \sum_{i=1}^{N_c} x_i \cdot b_i. \tag{10}$$

G_{∞}^{E} is the excess Gibbs free energy at infinite pressure,

$$\frac{G_{\infty}^{\mathrm{E}}}{RT} = \sum_{i=1}^{N_c} x_i \cdot \frac{\sum\limits_{j=1}^{N_c} \tau_{ji} b_j x_j C_{ji}}{\sum\limits_{k=1}^{N_c} b_k x_k C_{ki}}, \tag{11}$$

where

$$\tau_{ji} = \frac{g_{ji} - g_{ii}}{RT}, \tag{12}$$

$$g_{ji} - g_{ii} = \Delta g_{ji} \tag{13}$$

and

$$C_{ji} = \exp(-\alpha_{ji}\tau_{ji}). \tag{14}$$

For a second order Huron-Vidal, Δg_{ji} can be written as

$$\Delta g_{ji} = (d_{ji} + e_{ji} \cdot T + f_{ji} \cdot T^2) \cdot R, \tag{15}$$

where α_{ji} in Eq. 14 and d_{ji}, e_{ji} and f_{ji} in Eq. 15 are binary parameters to be fitted to experimental data. The used d, e, f and the non-randomness parameter α_{ji} for CO_2-water are listed in Table 1.

A general discussion was made by Kontogeorgis and Coutsikos (2012), who reviewed the 30 years development of the activity coefficient models that are incorporated for cubic EoSs.

[Table 1 about here.]

Here, for the ease of analysis and consistency with the work of Jørstad (1993), the molar based parameter $a_{\mathrm{n}} = a \cdot n^2$ is used instead, defined as

$$a_{\mathrm{n}} = b_{\mathrm{n}} \left(\sum_{i=1}^{N_c} \left(n_i \frac{a_i}{b_i} \right) - \frac{G^{\mathrm{E}}_{\infty \mathrm{n}}}{\ln(2)} \right), \tag{16}$$

where $b_{\mathrm{n}} = b \cdot n$ is defined as

$$b_{\mathrm{n}} = \sum_{i=1}^{N_c} n_i \cdot b_i \tag{17}$$

and $G^{\mathrm{E}}_{\infty \mathrm{n}} = G^{\mathrm{E}}_{\infty} \cdot n$.

Subsequently, the derivatives of a_{n} needed to calculate the scale factors can be easily derived as follows:

$$\frac{\partial a_{\mathrm{n}}}{\partial n_i} = b_i \cdot \frac{a_{\mathrm{n}}}{b_{\mathrm{n}}} + b_{\mathrm{n}} \left(\frac{a_i}{b_i} - \frac{1}{\ln(2)} \cdot \frac{\partial G^{\mathrm{E}}_{\infty \mathrm{n}}}{\partial n_i} \right) \tag{18}$$

$$\begin{aligned} \frac{\partial^2 a_{\mathrm{n}}}{\partial n_j \partial n_i} = {} & b_i \cdot \left(\frac{a_j}{b_j} - \frac{1}{\ln(2)} \cdot \frac{\partial G^{\mathrm{E}}_{\infty \mathrm{n}}}{\partial n_j} \right) + b_j \cdot \left(\frac{a_i}{b_i} - \frac{1}{\ln(2)} \cdot \frac{\partial G^{\mathrm{E}}_{\infty \mathrm{n}}}{\partial n_i} \right) \\ & - b_{\mathrm{n}} \cdot \frac{1}{\ln(2)} \cdot \frac{\partial^2 G^{\mathrm{E}}_{\infty \mathrm{n}}}{\partial n_j \partial n_i} \end{aligned} \tag{19}$$

$$\frac{\partial a_{\mathrm{n}}}{\partial T} = b_{\mathrm{n}} \left(\sum_{i=1}^{N_c} \left(\frac{n_i}{b_i} \cdot \frac{\partial a_i}{\partial T} \right) - \frac{1}{\ln(2)} \cdot \frac{\partial G^{\mathrm{E}}_{\infty \mathrm{n}}}{\partial T} \right) \tag{20}$$

$$\begin{aligned} \frac{\partial^2 a_{\mathrm{n}}}{\partial T \partial n_i} = {} & b_i \left(\sum_{i=1}^{N_c} \left(\frac{n_i}{b_i} \cdot \frac{\partial a_i}{\partial T} \right) - \frac{1}{\ln(2)} \cdot \frac{\partial G^{\mathrm{E}}_{\infty \mathrm{n}}}{\partial T} \right) \\ & + \frac{b_{\mathrm{n}}}{b_i} \cdot \frac{\partial a_i}{\partial T} - \frac{b_{\mathrm{n}}}{\ln(2)} \cdot \frac{\partial^2 G^{\mathrm{E}}_{\infty \mathrm{n}}}{\partial T \partial n_i} \end{aligned} \tag{21}$$

$$\frac{\partial^2 a_{\mathrm{n}}}{\partial T^2} = b_{\mathrm{n}} \left(\sum_{i=1}^{N_c} \left(\frac{n_i}{b_i} \cdot \frac{\partial^2 a_i}{\partial T^2} \right) - \frac{1}{\ln(2)} \cdot \frac{\partial^2 G^{\mathrm{E}}_{\infty \mathrm{n}}}{\partial T^2} \right) \tag{22}$$

Once the a_{n} and its derivatives are computed, the f_{n} and h_{n} and their derivatives can be computed.

3. Methodology

3.1. Numerical Tools

The NTNU-SINTEF in-house thermodynamic library was used for the study presented. The new model was integrated to the library framework. The library is a tool for predicting the thermodynamic properties using various approaches that ranges in level of sophistication and underlying theory. The tolerance used for this study was 10^{-4} for both the multi-phase flash algorithm and the compressibility factor calculations.

3.2. Error definition

The errors of an EoS are measured here by the Relative Error (RE) and the Average of Absolute Deviation (AAD) defined for an arbitrary variable C as

$$RE(C_r, \%) = \frac{|C_{\mathrm{s},r} - C_{\mathrm{exp},r}|}{C_{\mathrm{exp},r}} \times 100 \tag{23}$$

and

$$AAD(C, \%) = \frac{100}{N} \times \sum_{r=1}^{N} \frac{|C_{\mathrm{s},r} - C_{\mathrm{exp},r}|}{C_{\mathrm{exp},r}} \tag{24}$$

Here, N is the total number of points, subscripts s and exp refer to simulation data and experimental data, respectively, and r is a point index.

4. Results and discussion

4.1. Single phase density, high pressures

A set of conditions challenging for SPUNG and SRKs EoSs (Ibrahim et al., 2014b) at elevated pressures and various concentrations was evaluated using

the new EoS with the different reference fluids R23, R503 and NH_3. The tested concentrations varied from 90% CO_2 to 90% of H_2O over pressures that ranged from 10 to 100 MPa. The temperature at which the calculations were conducted was 400 °C. These conditions were consistent with the experimental data of Seitz and Blencoe (1999). The comparisons between the three tested reference fluids for the high-pressure data sets are plotted in Fig. 1. The figure shows the density change over molar fraction of CO_2 for the pressures of 14.94, 24.94, 39.94 and 99.93 MPa. The evaluation at low pressure data sets were excluded since all EoSs tested here and in Ibrahim et al. (2014b) were performing good for these conditions. This is obvious in Fig. 1 where at the lowest pressure of 14.94 MPa, all the new EoS and SPUNG EoS were very accurate over the entire range of concentrations.

[Figure 1 about here.]

The results showed very good matching and an improvement compared to SPUNG and SRKs EoSs results presented by Ibrahim et al. (2014b), especially as the pressure went up to 99.93 MPa. The mixing rules do not play a significant role, especially for single phase, because they influence only the a parameter calculations. Hence, improvement is argued to be mainly due to the use of the Bender 20 parameters MBWR EoS of Polt (1987) with the reference fluids R23, R503 and NH_3.

4.2. Rich phases

The new EoS was evaluated at conditions consistent with the experiments of Chiquet et al. (2007), King et al. (1992) and Hebach et al. (2004). Chiquet et al. (2007) measured densities of both CO_2-rich and water-rich

phases when the CO_2-rich one was supercritical. The experiments were conducted at pressures that varied from 5 to 45 MPa, and the temperatures of CO_2-rich phases presented here were 35, 50, 90 and 110 °C. King et al. (1992) measured water-rich liquid-phase densities at pressures between 6 to 24 MPa. The temperatures at which the experiments were conducted were 15, 20, and 25 °C. The co-existing phase was CO_2-rich liquid phase. Hebach et al. (2004) data were used to evaluate the EoS for predicting water-rich liquid phase densities co-existing with CO_2-rich gas phase. The results of Chiquet et al. (2007) and Hebach et al. (2004) were measured at temperatures slightly around the listed values, although precisely fixed for each point.

The Supercritical Liquid Equilibrium (SGLE) CO_2-rich phase density predictions using the new EoS are presented in comparison to SPUNG and with the experimental data of Chiquet et al. (2007) in Fig. 2. The AAD of these predictions are shown in Table 2.

[Figure 2 about here.]

[Table 2 about here.]

The density predictions using the new EoS of the liquid water-rich phase co-existing with a supercritical CO_2-rich phase at a temperature of 35 °C are presented in comparison with the experimental data of Chiquet et al. (2007) in Fig. 3.

[Figure 3 about here.]

The King et al. (1992) densities of the liquid water-rich phase co-existing with liquid CO_2-rich phase at a temperature of 15 °C are compared to the

new EoS and SPUNG EoS in Fig. 4. Due to the similarity in trend between the results of 25 °C and 15 °C, the former are not shown here.

[Figure 4 about here.]

Density predictions using the new EoS of the liquid water-rich phase coexisting with gaseous CO_2-rich phase at a temperature of 29 °C are plotted in Fig. 5. The comparison at 19, 39 and 49 °C were similar, thus not presented here.

[Figure 5 about here.]

[Table 3 about here.]

Using the new EoS, the results for the CO_2-rich phase are slightly overshooting. However, the water-rich phase density predictions became very accurate. This can be attributed to the use of the reference fluids R23, R503 and NH_3. The results imply that R23 is the best compromise when CO_2-water is of concern.

4.3. Solubilities

The accuracies of the new EoS in predicting the mutual solubilities of CO_2 and H_2O were validated against experimental data.

A review of the experimental data of CO_2-water system solubilities was given by Pappa et al. (2009). They recommended six sets of mutual solubilities data for model regression and validation. These six sets were those of Valtz et al. (2004), Mueller et al. (1988), Bamberger et al. (2000), King et al. (1992), Takenouchi and Kennedy (1964) and Wiebe (1941). The recent work by Hou et al. (2013) covered the available intermediate pressure

data available in literature at various temperatures and, in addition, filled in some gaps. Hou et al. (2013) also compared the new data against those of the literature and found very good match. Takenouchi and Kennedy (1964) presented solubilities for very high pressures (10 to 70 MPa) between 110 and 350 °C. We only evaluated data at 110 °C, as higher temperatures are of minor relevance for CCS. Wiebe (1941) presented own data and data from Wiebe and Gaddy (1939) for the pressure range of 1 to 70 MPa at temperatures from 25 to 100 °C. Owing to the fact that mutual solubility values were presented only for 75 and 100 °C, our calculations are limited to these data sets. The study of Bamberger et al. (2000) covered only pressures from 4 to 14 MPa at 50, 60, and 80 °C temperature values. The work of Valtz et al. (2004) investigated very low pressures at about 5, 25, and 45 °C. At 5 °C they measured pressures from 0.5 to 1 MPa. The pressures ranged approximately between 0.5 and 1 MPa. The span became wider as the temperature increased. At 45 °C, it was about 0.1 to 7 MPa. Mueller et al. (1988) published solubilities for another range; namely low pressures in conjunction with high temperatures (100 - 200 °C). The last study we compared with was Hou et al. (2013), which covered a large range of data for pressure values 1 - 17.5 MPa in conjunction with temperature values 25 - 175 °C.

We assessed the proposed EoS by comparing the predictions to SPUNG EoS and with the experimental works cited above. Fig. 6 shows our results with the data of Valtz et al. (2004). In addition, we assessed the solubilities at 25 °C, which yielded results similar to those shown in the figure. Table 4 gives the associated AADs.

[Figure 6 about here.]

[Table 4 about here.]

Fig. 7 shows our results compared with Mueller et al. (1988) experimental data. In this figure we skipped the interim temperature, owing to the fact that those plotted were sufficient to illustrate the trend. However, Table 8 shows the AADs for the three assessed temperatures.

[Figure 7 about here.]

[Table 5 about here.]

[Figure 8 about here.]

[Table 6 about here.]

For moderate pressures we chose the conditions to model according to Bamberger et al. (2000). Fig. 8 shows the comparison between our results and their experimental data, while Table 6 presents the AADs. We compare our results with the data of King et al. (1992) and of Hou et al. (2013) in Fig. 9 and Fig. 10, respectively. Interim temperatures were left out with the same rationale as in the comparisons above. Table 8 summarizes AADs with respect to temperature. Fig. 12 and Table 9 compare our results with those of Wiebe (1941) experiments.

[Figure 9 about here.]

[Table 7 about here.]

[Figure 10 about here.]

[Figure 11 about here.]

[Table 8 about here.]

[Figure 12 about here.]

[Table 9 about here.]

The proposed EoS was used to predict the mutual solubilities of CO_2 and H_2O at very high pressures. The conditions are consistent with the work of Takenouchi and Kennedy (1964), namely between 10 MPa and 70 MPa, in conjunction with a temperature of 110 °C. Fig. 13 and Table 10 show our results and errors (in terms of AADs), respectively, with reference to the work of Takenouchi and Kennedy (1964).

[Figure 13 about here.]

[Table 10 about here.]

4.4. General discussion

The new EoS predicted the phase equilibrium very accurately. The comparison to SPUNG EoS showed large improvements. This is because the HV mixing rules has the advantage of handling asymmetric polar mixtures like CO_2-water, contrary to the symmetric quadratic mixing rule of van der Waals used in SPUNG EoS. We choose to derive the HV mixing rule for the shape factors calculation as it has the advantage of being a consistent mixing rule unlike the other asymmetric mixing rules that has the Michelsen-Kistenmacher syndrome (Michelsen and Kistenmacher, 1990). Moreover, in combination with the usage of the Bender-MBWR EoS parameters of Polt (1987) and the tested reference fluids, the new EoS predicted both densities and phase equilibrium for the polar mixture of CO_2-water accurately using the same set of parameters. The new EoS is of the same order of computational complexity as the SPUNG EoS. Therefore, the new ECS EoS

is a similar compromise between computational time and accuracy. This achievements make the new EoS readily usable by CCS industry for its high accuracy and reasonable computational time.

5. Conclusions

A thermodynamically consistent extended corresponding states (ECS) EoS was developed for CCS industry. The new EoS can handle the phase equilibrium of the polar mixtures of CO_2-water with high accuracy. The high accuracy when compared with experimental data is achieved over a wide range of pressures and temperatures. This achievement is due to the proposed development of a Huron-Vidal mixing rules based approach of computing the scale factors. The usage of R23, R503 and NH_3 as reference fluids allowed simultaneous accurate predictions of the density and phase equilibrium of the CO_2-water systems. This is achieved for single phase at high pressures, supercritical-liquid, liquid-liquid, and vapor-liquid equilibrium.

Acknowledgement: This work was financed through the CO2 Dynamics project. The authors acknowledge the support from the Research Council of Norway (189978), Gassco AS, Statoil Petroleum AS and Vattenfall AB.

References

Bamberger, A., Sieder, G., Maurer, G., 2000. High-pressure (vapor+liquid) equilibrium in binary mixtures of (carbon dioxide+water or acetic acid)

at temperatures from 313 to 353 K. J. Supercrit. Fluids, 17(2), 97 – 110.

Chapman, W.G., Gubbins, K.E., Jackson, G., Radosz, M., 1990. New reference equation of state for associating liquids. Ind. Eng. Chem. Res., 29(8), 1709–1721.

Chiquet, P., Daridon, J.L., Broseta, D., Thibeau, S., 2007. CO_2/water interfacial tensions under pressure and temperature conditions of CO_2 geological storage. Energy Convers. Manage., 48(3), 736 – 744.

Diamantonis, N.I., Economou, I.G., 2012. Modeling the phase equilibria of a H_2O-CO_2 mixture with PC-SAFT and tPC-PSAFT equations of state. Mol. Phys., 110(11-12), 1205–1212.

Ely, J.F., 1990. A predictive, exact shape factor extended corresponding states model for mixtures. Adv. Cryog. Eng., 35, 1511–1520.

Estela-Uribe, J.F., Trusler, J.P.M., 1998. Shape factors for the light hydrocarbons. Fluid Phase Equilib., 150-151, 225 – 234.

Fisher, G.D., Leland, T.W., 1970. Corresponding states principle using shape factors. Ind. Eng. Chem. Fundam., 9(4), 537–544.

Hebach, A., Oberhof, A., Dahmen, N., 2004. Density of water + carbon dioxide at elevated pressures: measurements and correlation. J. Chem. Eng. Data, 49(4), 950–953.

Hou, S.X., Maitland, G.C., Trusler, J.M., 2013. Measurement and modeling of the phase behavior of the (carbon dioxide + water) mixture at temperatures from 298.15 K to 448.15 K. J. Supercrit. Fluids, 73, 87–96.

Huron, M.J., Vidal, J., 1979. New mixing rules in simple equations of state for representing vapour-liquid equilibria of strongly non-ideal mixtures. Fluid Phase Equilib., 3(4), 255 – 271.

Ibrahim, M., Skaugen, G., Ertesvåg, I.S., 2012. Preliminary evaluation of the SPUNG equation of state for modelling the thermodynamic properties of CO_2- water mixtures. Energy Procedia, 26, 90 – 97.

Ibrahim, M., Skaugen, G., Ertesvåg, I.S., 2014a. Modelling CO_2 water thermodynamics using spung equation of state (EoS) concept with various reference fluids. Energy Procedia, In press.

Ibrahim, M., Skaugen, G., Ertesvåg, I.S., Haug-Warberg, T., 2014b. Modelling CO_2 - water mixture thermodynamics using various equations of state (EoS) with emphasis on the potential of the SPUNG EoS. Chem. Eng. Sci., 113, 22 – 34.

Jørstad, O., 1993. Equations of state for hydrocarbon mixtures. Dr. Ing. thesis No. NTH 1993:92. Norwegian Inistitute of Technology, Trondheim, Norway.

King, M.B., Mubarak, A., Kim, J.D., Bott, T.R., 1992. The mutual solubilities of water with supercritical and liquid carbon dioxides. J. Supercrit. Fluids, 5(4), 296 – 302.

Kontogeorgis, G.M., Coutsikos, P., 2012. Thirty years with eos/ge modelswhat have we learned? Ind. Eng. Chem. Res., 51(11), 4119–4142.

Kontogeorgis, G.M., Voutsas, E.C., Yakoumis, I.V., Tassios, D.P., 1996. An equation of state for associating fluids. Ind. Eng. Chem. Res., 35(11), 4310–4318.

Kunz, O., Klimeck, R., Wagner, W., Jaeschke, M., 2007. The GERG-2004 Wide-Range Equation of State for Natural Gases and Other Mixtures. GERG TM15, VDI Verlag, Düsseldorf, Germany.

Leach, J.W., Chappelear, P.S., Leland, T.W., 1968. Use of molecular shape factors in vapor-liquid equilibrium calculations with the corresponding states principle. AIChE J., 14(4), 568–576.

Michelsen, M.L., Kistenmacher, H., 1990. On composition-dependent interaction coefficeints. Fluid Phase Equilib., 58(12), 229 – 230.

Michelsen, M., Mollerup, J., 2007. Thermodynamic Models: Fundamentals & Computational Aspects. Tie-Line Publications.

Mollerup, J., 1998. Unification of the two-parameter equation of state and the principle of corresponding states. Fluid Phase Equilib., 148(1-2), 1–19.

Mueller, G., Bender, E., Maurer, G., 1988. Das Dampf-fluessigkeitsgleichgewicht des ternaeren Systems Ammonik-Kohlendioxid-Wasser bei hohn Wassergehalten im Bereich zwischen 373 und 473 Kelvin. Ber. Bunsenges. Phys. Chem., 92, 148–160.

Pappa, G.D., Perakis, C., Tsimpanogiannis, I.N., Voutsas, E.C., 2009. Thermodynamic modeling of the vapor-liquid equilibrium of the CO2/H2O mixtures. Fluid Phase Equilib., 284(1), 56–63.

Peng, D.Y., Robinson, D.B., 1976. A new two-constant equation of state. Ind. Eng. Chem. Fundam., 15(1), 59–64.

Polt, A., 1987. Zur beschreibung der thermodynamischen eigenschaften reiner fluide mit "Erweiterten BWR-Gleichungen". Dissertation.

Seitz, J.C., Blencoe, J.G., 1999. The CO2-H2O system. I. Experimental determination of volumetric properties at 400°C, 10-100 MPa. Geochim. Cosmochim. Acta, 63(10), 1559 – 1569.

Soave, G., 1972. Equilibrium constants from a modified Redlich-Kwong equation of state. Chem. Eng. Sci., 27(6), 1197 – 1203.

Span, R., Wagner, W., 1996. A new equation of state for carbon dioxide covering the fluid region from the tripple-point temperature to 1100 K at pressures up to 800 MPa. J. Phys. Chem. Ref. Data, 25(6), 1509–1596.

Takenouchi, S., Kennedy, G.C., 1964. The binary system H_2O-CO_2 at high temperatures and pressures. Am. J. Sci., 262(9), 1055–1074.

Tsivintzelis, I., Kontogeorgis, G.M., Michelsen, M.L., Stenby, E.H., 2011. Modeling phase equilibria for acid gas mixtures using the CPA equation of state. Part II: Binary mixtures with CO_2. Fluid Phase Equilib., 306(1), 3856.

Valtz, A., Chapoy, A., Coquelet, C., Paricaud, P., Richon, D., 2004. Vapour-liquid equilibria in the carbon dioxide-water system, measurement and modelling from 278.2 to 318.2 K. Fluid Phase Equilib., 226, 333 – 344.

Wiebe, R., 1941. The binary system carbon dioxide-water under pressure. Chem. Rev., 29(3), 475–481.

Wiebe, R., Gaddy, V., 1939. The solubility in water of carbon dioxide at 50, 75 and 100 °, at pressures to 700 atmospheres. J. Am. Chem. Soc., 61(2), 315–318.

Wilhelmsen, Ø., Skaugen, G., Jørstad, O., Li, H., 2012. Evaluation of

SPUNG and other equations of state for use in carbon capture and storage modelling. Energy Procedia, 23, 236 – 245.

List of figures caption:

Figure 1. Single Phase density computations in comparison with experimental data of Seitz and Blencoe (1999), over mole fractions of CO_2 at different pressures and a temperature of 400 °C.

Figure 2. SGLE CO_2-rich phase density predictions at temperatures about 35, 50, 90 and 110 °C in comparison with Chiquet et al. (2007) experimental data.

Figure 3. Densities of the liquid water-rich phase co-existing with a supercritical CO_2-rich phase at a temperature about 35 °C in comparison with Chiquet et al. (2007) experimental data.

Figure 4. LLE water-rich phase density predictions at a temperature 15 °C in comparison with King et al. (1992) experimental data.

Figure 5. Densities of the liquid water-rich phase co-existing with a gaseous CO_2-rich phase at a temperature about 29 °C in comparison with Hebach et al. (2004) experimental data.

Figure 6. CO_2 and H_2O solubilities over low pressures and at temperatures of 5 and 45 °C in comparison with Valtz et al. (2004) experimental data.

Figure 7. CO_2 and H_2O solubilities over low pressures and at temperatures of 100 and 200 °C in comparison with Mueller et al. (1988) experimental data.

Figure 8. CO_2 and H_2O solubilities over moderate pressures and at temperature of 50 and 80 °C in comparison with Bamberger et al. (2000) experimental data.

Figure 9. CO_2 solubilities over moderate pressures and at temperatures of

15 and 50 °C in comparison with King et al. (1992) experimental data.

Figure 10. CO_2 solubilities computations in comparison with experimental data of Hou et al. (2013).

Figure 11. H_2O solubilities computations in comparison with experimental data of Hou et al. (2013).

Figure 12. CO_2 and H_2O solubilities over moderate pressures and at temperatures of 50 and 75 °C in comparison with Wiebe (1941) experimental data.

Figure 13. CO_2 and H_2O solubilities over very high pressures and a temperature of 110 °C in comparison with Takenouchi and Kennedy (1964) experimental data.

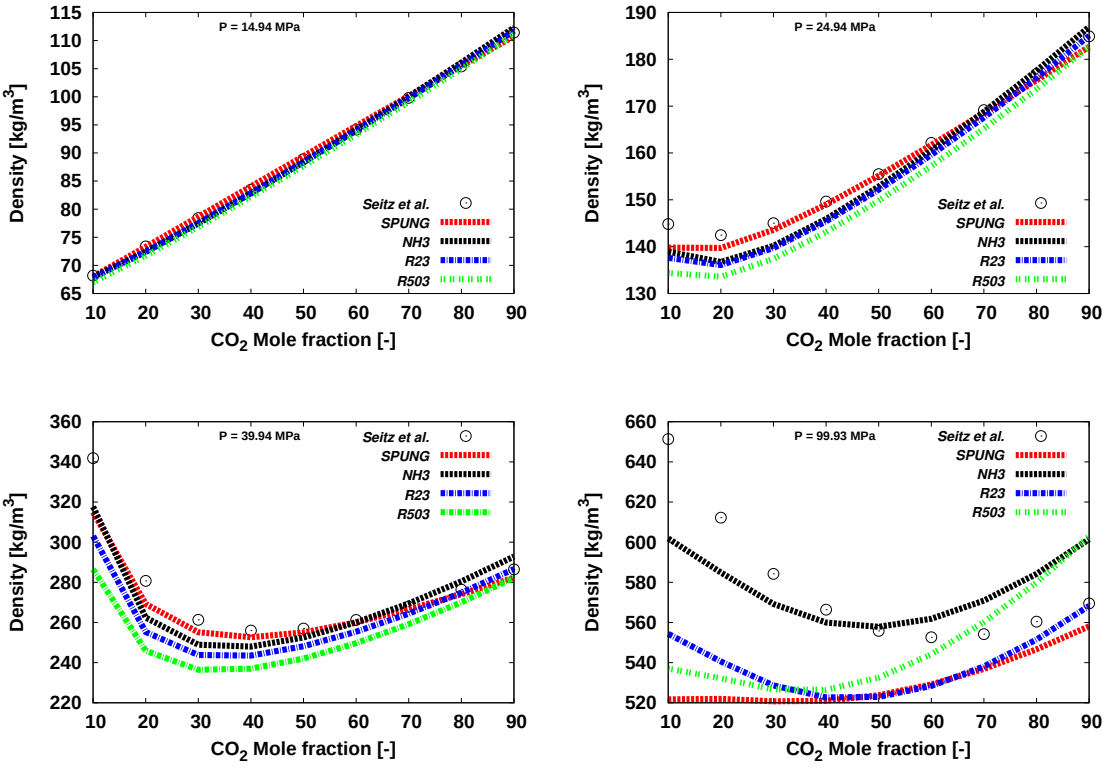

Figure 1: Single phase density computations in comparison with experimental data of Seitz and Blencoe (1999), over mole fractions of CO_2 at different pressures and a temperature of 400 °C

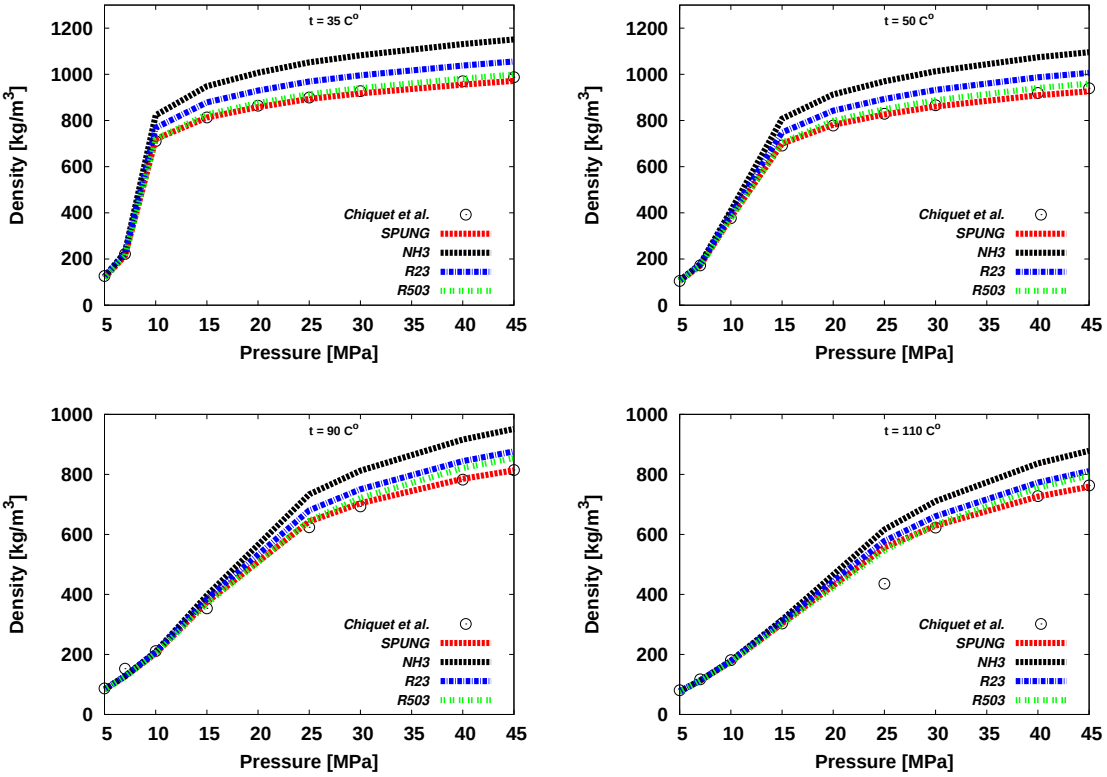

Figure 2: SGLE CO_2-rich phase density predictions at temperatures about 35, 50, 90 and 110 °C in comparison with Chiquet et al. (2007) experimental data

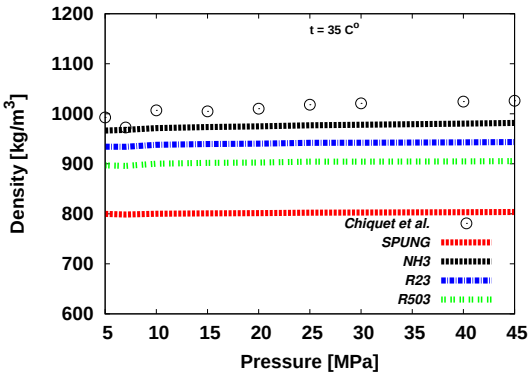

Figure 3: Densities of the liquid water-rich phase co-existing with a supercritical CO_2-rich phase at a temperature about 35 °C in comparison with Chiquet et al. (2007) experimental data

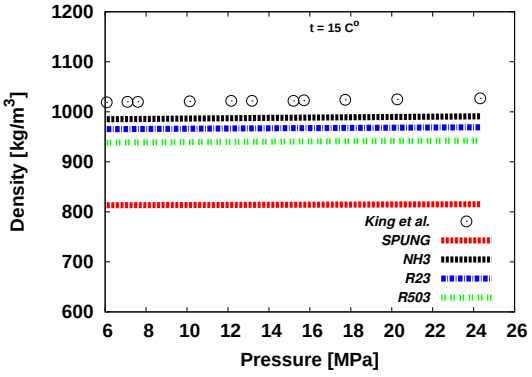

Figure 4: LLE water-rich phase density predictions at a temperature 15 °C in comparison with King et al. (1992) experimental data

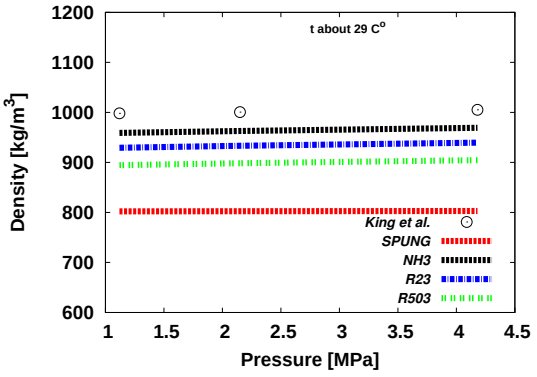

Figure 5: Densities of the liquid water-rich phase co-existing with a gaseous CO_2-rich phase at a temperature about 29 °C in comparison with Hebach et al. (2004) experimental data

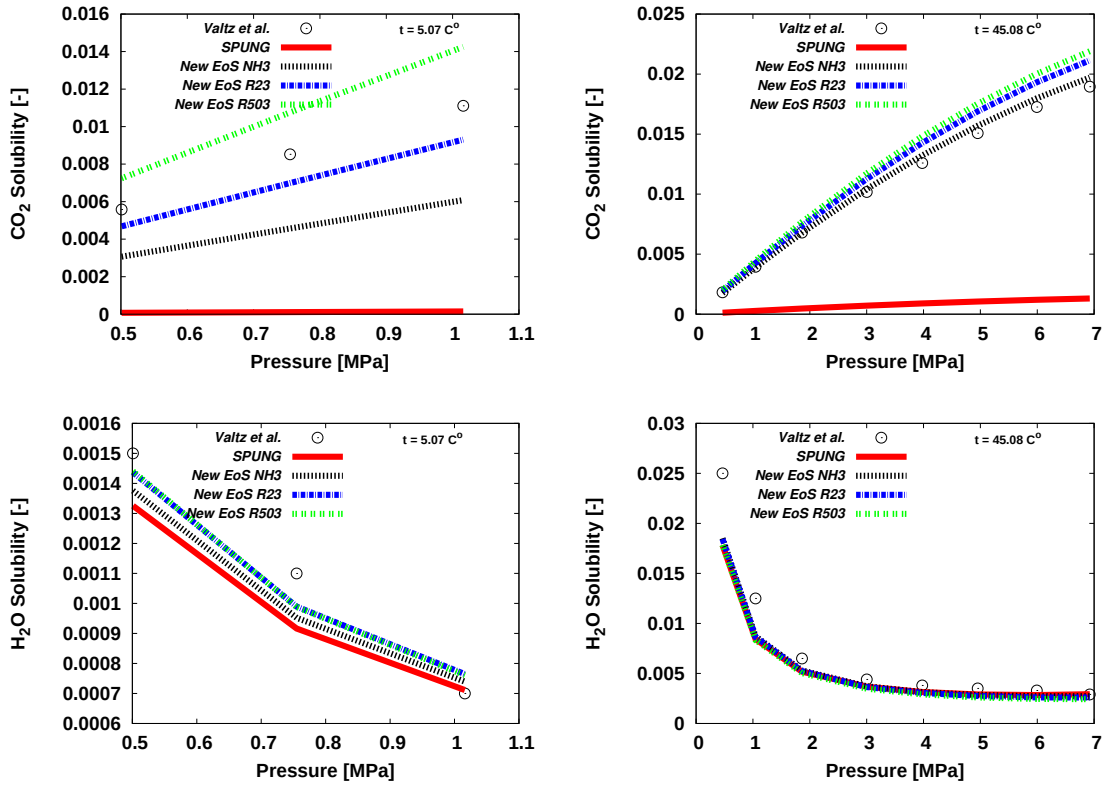

Figure 6: CO_2 and H_2O solubilities over low pressures and at temperatures of about 5 and 45 °C in comparison with Valtz et al. (2004) experimental data

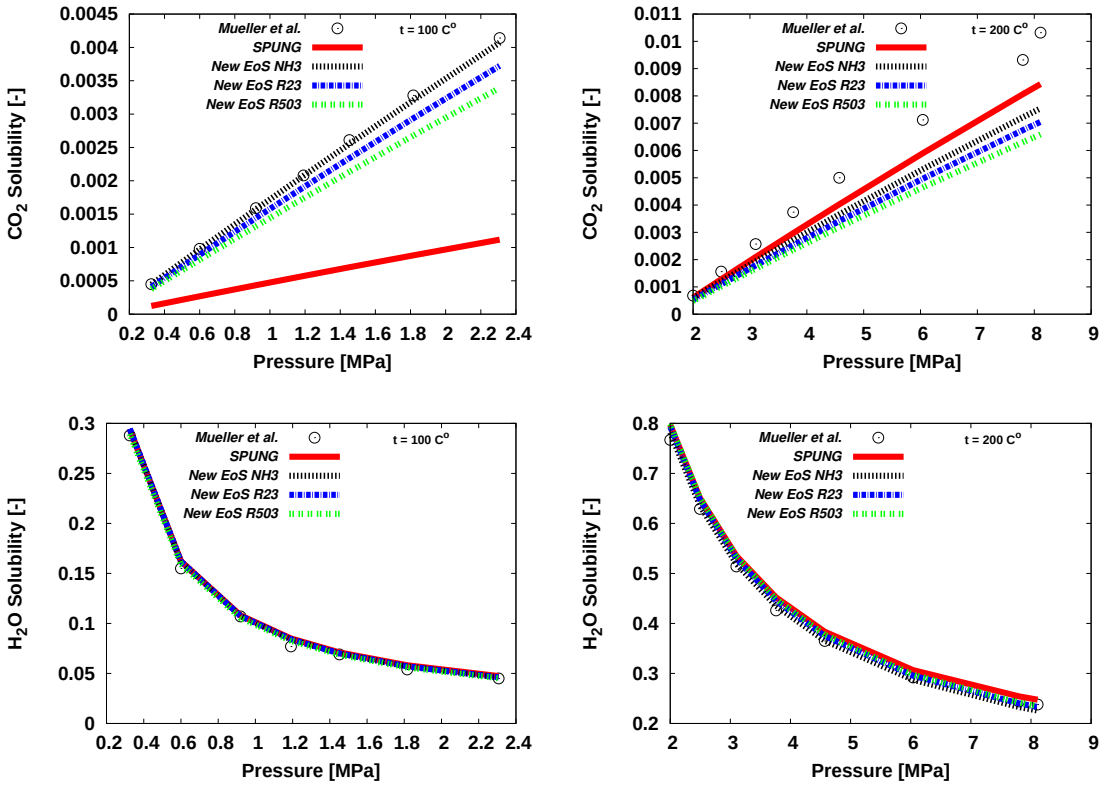

Figure 7: CO_2 and H_2O solubilities over low pressures and at temperatures of 100 and 200 °C in comparison with Mueller et al. (1988) experimental data

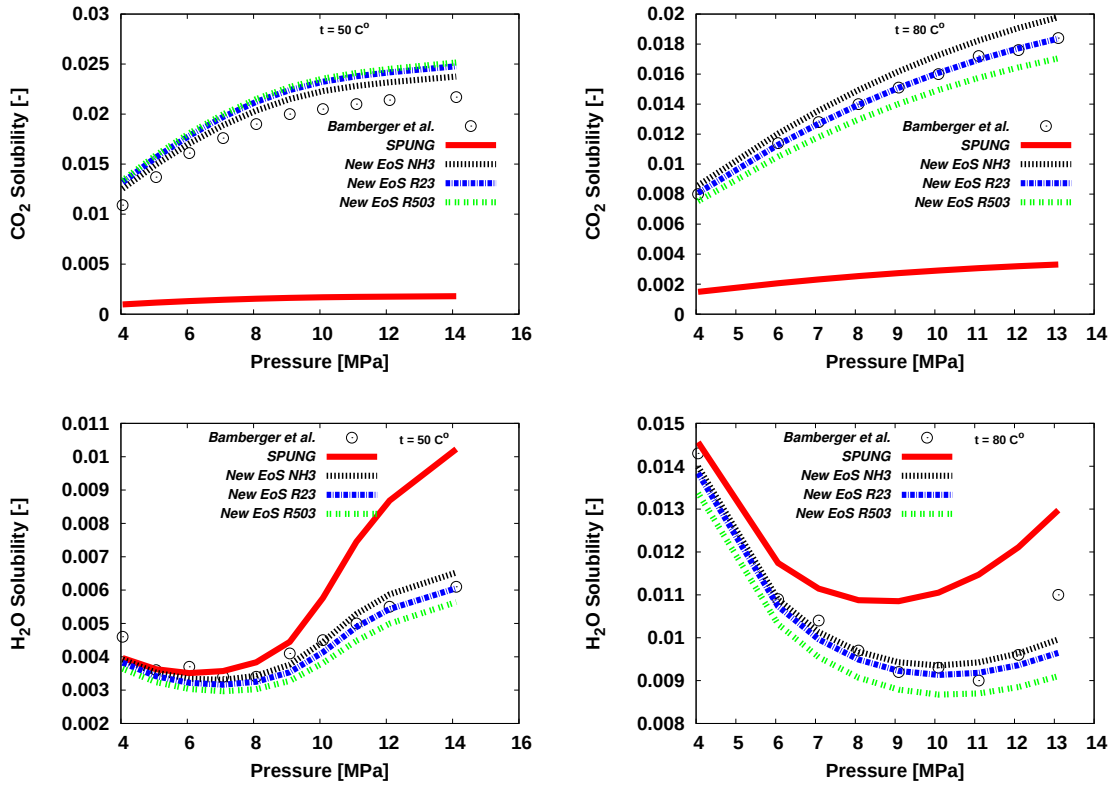

Figure 8: CO_2 and H_2O solubilities over moderate pressures and at temperatures of 50 and 80 °C in comparison with Bamberger et al. (2000) experimental data

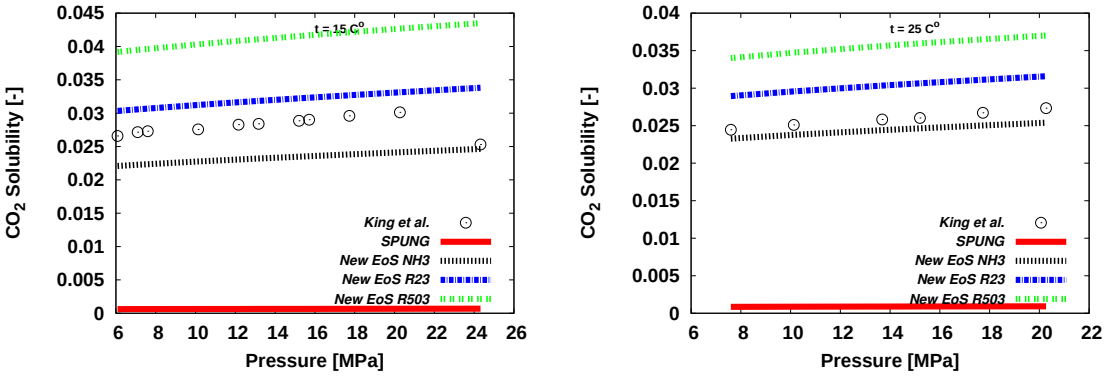

Figure 9: CO_2 solubilities over moderate pressures and at temperatures of 15 and 50 °C in comparison with King et al. (1992) experimental data

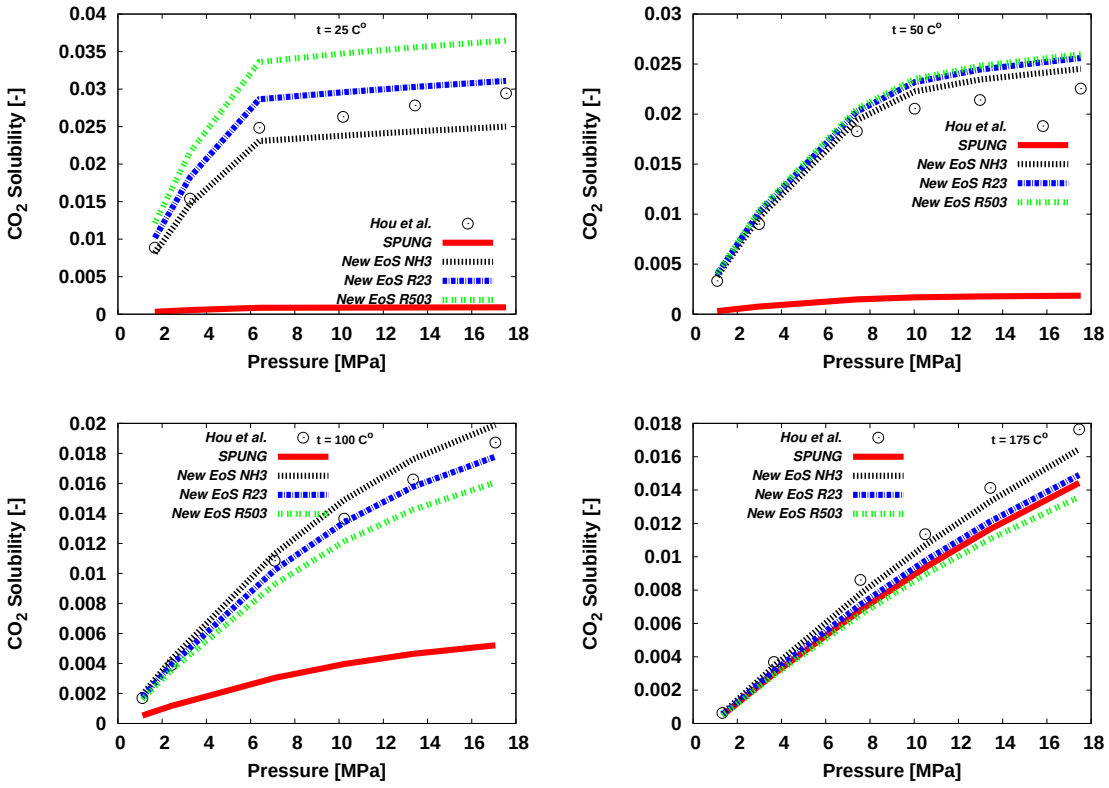

Figure 10: CO_2 solubilities computations in comparison with experimental data of Hou et al. (2013)

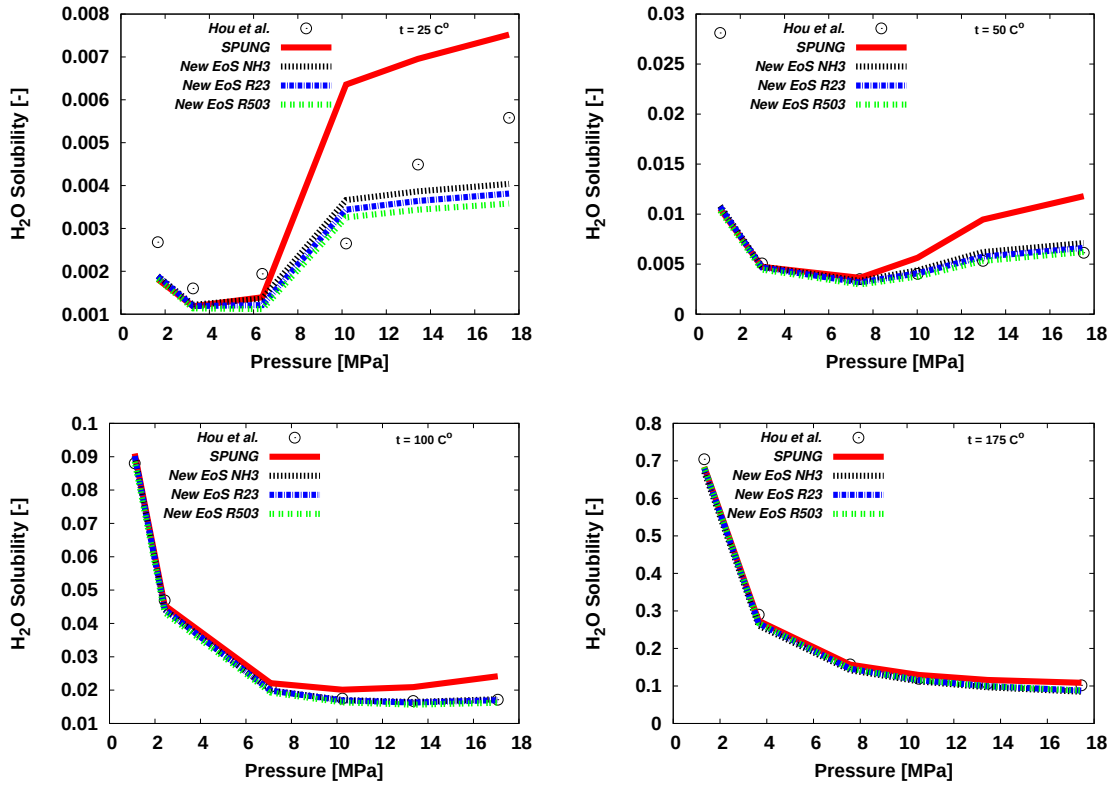

Figure 11: H_2O solubilities computations in comparison with experimental data of Hou et al. (2013)

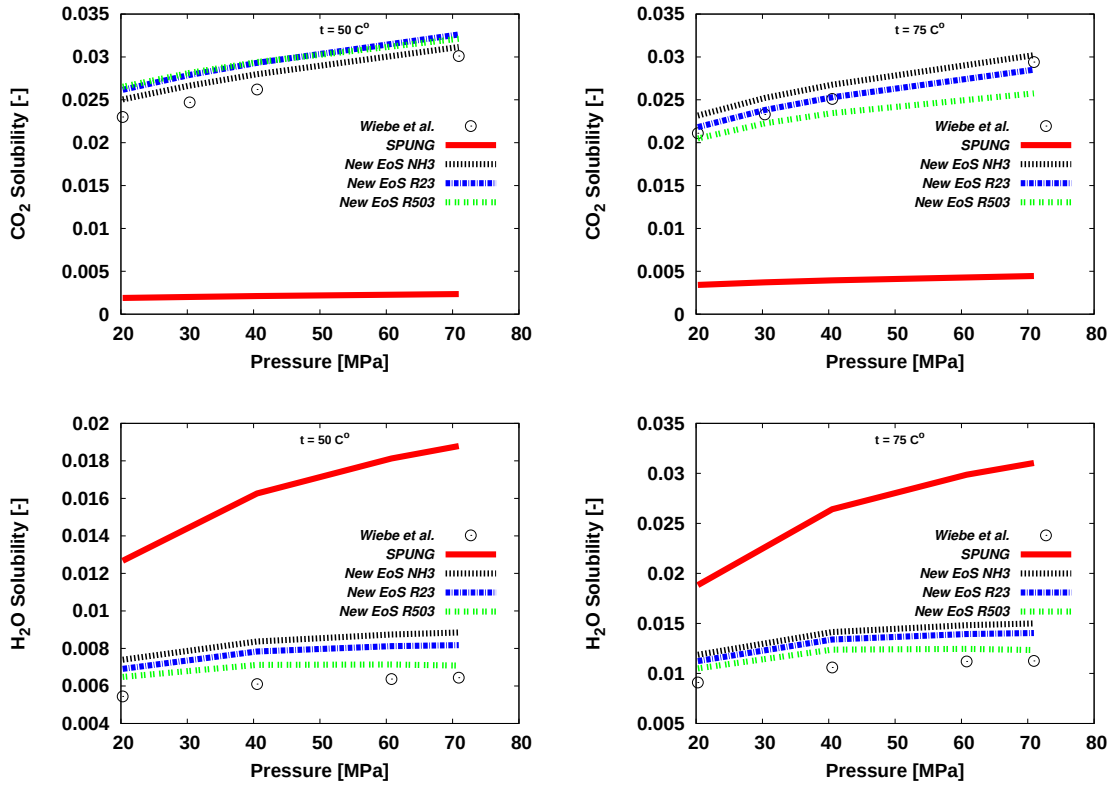

Figure 12: CO_2 and H_2O solubilities over moderate pressures and at temperatures of 50 and 75 °C in comparison with Wiebe (1941) experimental data

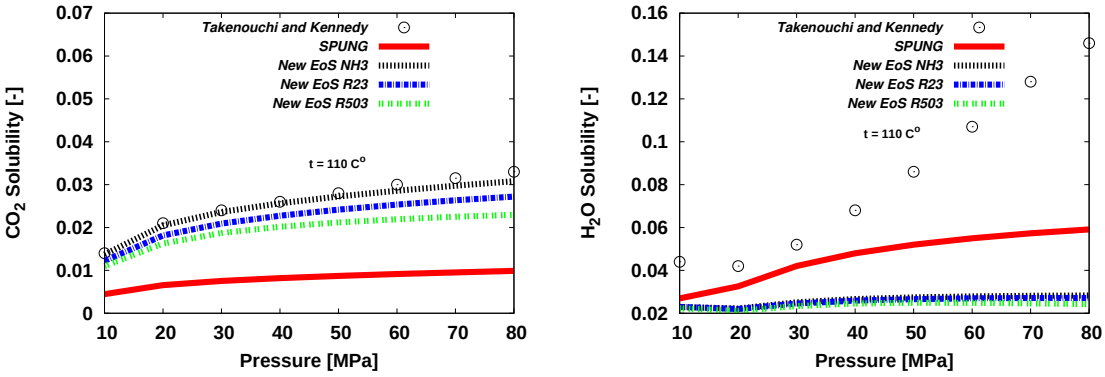

Figure 13: CO_2 and H_2O solubilities over very high pressures and a temperature of 110 °C in comparison with Takenouchi and Kennedy (1964) experimental data

Table 1: The d, e, f and α values used for this study, where component i is CO_2 and j is water

d_{ji}	e_{ji}	f_{ji}	d_{ij}	e_{ij}	f_{ij}	α_{ji}
-1035.17623	17.07660	0.03200	5887.42379	1.75852	-0.01513	0.03

Table 2: AAD [%] of the CO_2-rich phases density calculations for the CO_2-water system at different temperatures

Data sets	Phase Equilibrium	Temperature [°C]	SPUNG	NH3	R23	R503
Chiquet et al. (2007)	SGLE					
		35	1.8	13.5	6.3	2.1
		50	0.7	12.8	6.0	1.7
		70	2.0	13.0	6.9	3.2
		90	4.5	12.7	7.9	5.9
		110	5.3	12.4	7.9	6.2

Table 3: AAD [%] of water rich liquid phase densities averaged over the temperatures of each evaluated set of data

Data sets	Phase Equilibrium	SPUNG	NH3	R23	R503
King et al. (1992)	LLE	20.5	3.4	5.8	8.8
Chiquet et al. (2007)	SGLE	21.6	5.3	9.9	14.7
Hebach et al. (2004)	VLE	20.1	4.3	7.2	8.7

Table 4: AAD [%] of the solubility of CO_2 and H_2O in comparison with Valtz et al. (2004)

Component	Temperature [°C]	SPUNG	NH3	R23	R503
CO_2	5.07	98.7	45.6	16.8	28.1
	25.13	96.8	15.9	4.9	25.0
	45.08	93.1	3.0	10.2	14.7
H_2O	5.07	10.0	9.1	7.8	7.6
	25.13	17.8	15.4	15.4	18.1
	45.08	17.5	18.7	20.8	24.6

Table 5: AAD [%] of the solubility of CO_2 and H_2O in comparison with Mueller et al. (1988)

Component	Temperature [°C]	SPUNG	NH3	R23	R503
CO_2	100	72.8	1.3	9.5	17.3
	140	49.2	8.2	17.3	25.1
	200	17.0	23.6	29.5	34.4
H_2O	100	4.9	3.7	3.8	2.3
	140	3.1	5.8	4.5	5.0
	200	4.5	2.2	2.7	3.0

Table 6: AAD [%] of the solubility of CO_2 and H_2O in comparison with Bamberger et al. (2000)

Component	Temperature [°C]	SPUNG	NH3	R23	R503
CO_2	50	91.7	8.7	13.6	15.2
	60	88.9	9.9	9.5	7.0
	80	81.9	7.0	0.7	7.2
H_2O	50	24.7	5.9	7.2	13.5
	60	20.5	5.9	5.7	9.9
	80	15.2	2.5	3.3	7.4

Table 7: AAD [%] of the solubility of CO_2 at different temperatures in comparison with King et al. (1992)

Temperature [°C]	SPUNG	NH3	R23	R503
15	97.0	17.0	14.0	47.0
20	97.2	11.5	15.4	41.4
25	96.6	5.7	17.2	37.6

Table 8: AAD [%] of the solubility of CO_2 and H_2O in comparison with Hou et al. (2013)

Component	Temperature [°C]	SPUNG	NH3	R23	R503
CO_2	25	96.6	9.5	12.6	32.7
	50	91.6	8.9	14.1	15.9
	75	82.9	13.3	7.5	2.4
	100	70.9	8.5	3.3	11.0
	125	57.4	2.3	12.0	21.0
	150	39.8	6.8	15.1	23.3
	175	19.3	6.9	15.3	22.5
H_2O	25	52.7	27.1	28.9	30.9
	50	47.1	19.0	16.0	16.4
	75	24.4	4.6	3.5	4.8
	100	15.5	3.1	3.4	5.8
	125	12.0	5.7	4.8	6.5
	150	6.7	10.3	8.4	9.0
	175	5.5	9.5	7.0	6.8

Table 9: AAD [%] of the solubility of CO_2 and H_2O at different temperatures in comparison with Wiebe (1941)

Component	Temperature [°C]	SPUNG	NH3	R23	R503
CO_2	50	92.0	6.8	11.7	12.0
	75	84.3	6.8	2.4	6.6
H_2O	50	167.9	37.0	27.5	14.5
	75	148.0	32.4	24.8	13.3

Table 10: AAD [%] of solubilities in comparison with Takenouchi and Kennedy (1964)

Component	SPUNG	NH3	R23	R503
CO_2	68.9	3.4	14.3	24.8
H_2O	36.2	63.6	64.3	66.3